Effect of Polymer Structure and Incorporation of Nanoparticles on the Behavior of Syndiotactic Polypropylenes

Julian Bejarano, Rosario Benavente, Ernesto Pérez, Manfred Wilhelm, Raúl Quijada, Humberto Palza*

A syndiotactic polypropylene (sPP) homopolymer and its copolymer with 1.4 mol% of norbornene (NsPP) are synthesized using a metallocene catalyst and the effect on the main properties of the addition of 4 wt% of either silica nanoparticles or multiwalled carbon nanotubes (CNTs) is studied. Important changes are observed in the thermal behavior of the different samples, primarily related to a strong nucleating effect of the nanofillers, much larger in CNTs than in silica, and to cold crystallization processes in the copolymer. Moreover, a rather relevant effect of the nanoparticles and their type, and of the cyclic comonomer is observed on the mechanical behavior of the polymer in the solid state. A strong effect of the kind of nanoparticle is also observed in the melt rheological properties of the samples, where again CNTs render larger changes than silica nanoparticles. On the contrary, oxygen permeation of sPP is unchanged with the addition of nanoparticles.

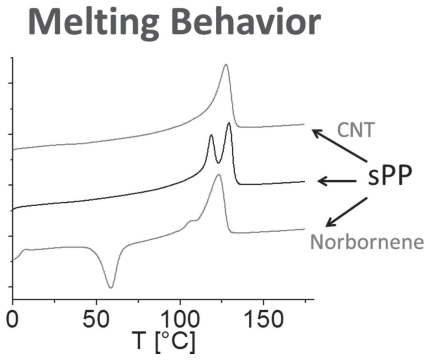

1. Introduction

Polyolefins are nowadays one of the most important plastic materials due to their excellent cost/performance value, low density, and easy recyclability and processability, representing more than 50 vol% of all commercial polymers.[1,2] The reason of this high production is the steady development and improvement of catalytic systems allowing the synthesis of polymer chains with tailored microstructures or configurations, such as either polypropylenes with controlled tacticities or polyethylenes with different branching or topologies[3,4] This morphological control allows the use of polyolefins in several applications replacing materials with higher densities and costs, thus explaining the steady production growth during the last 40 years.[1] Today the market of polyolefins is mostly based on polyethylenes and isotactic polypropylenes (iPP), although there is an opportunity to use other kinds of materials such as syndiotactic polypropylenes (sPP). sPP is an excellent candidate to further extend the range of applications of polyolefins because of its good properties such as higher impact resistance, better adhesion to difference surfaces, clarity, heat sealability, tear strength, tolerance to high energy radiation, oxidative degradation, and thermoplastic-elastomeric behavior[5,6]

J. Bejarano, Prof. R. Quijada, Dr. H. Palza
Departamento de Ingenieria Quimica y Biotecnologia, Facultad de Ciencias Fisicas y Matematicas, Universidad de Chile, Beauchef 861, Casilla 277, Santiago, Chile
E-mail: hpalza@ing.uchile.cl
Dr. R. Benavente, Dr. E. Pérez
Instituto de Ciencia y Tecnología de Polímeros (CSIC), Juan de la Cierva 3, 28006-Madrid, Spain
Prof. M. Wilhelm
Karlsruhe Institute of Technology (KIT), Department of Chemistry and Bioscience, Institute of Chemical Technology and Polymerchemistry, Engesserstrasse 18, 76131 Karlsruhe, Germany

DOI: 10.1002/macp.201300392

Despite the excellent properties of polyolefins, the lack of chemical functionalities in their chains reduces its compatibility with other materials, limiting its applications and behavior. The introduction of functionality into the main chain of polyolefins allows the preparation of new polymers with enhanced chemical and physical properties such as adhesion, dyeability, printability, and compatibility with other polymers.[7] A suitable route to incorporate functional groups in polyolefins is by adding cyclic groups in the main chain that can be modified by post-reactor reactions[8,9] Ziegler–Natta and other traditional olefin polymerization catalytic systems are unable to incorporate cyclic or functional olefins into the polymer chain, whereas metallocenes can add these molecules into the backbone with high activities.[10,11] These cyclic olefin copolymers (COCs) are further attractive materials since they can exhibit high transparency and glass transition temperatures (T_gs), good chemical and heat resistance, and good processability.[11] Another characteristic of these materials is the control of the T_g that can be increased depending on the amount of cyclic comonomer.[11] Previous results showed that the synthesis of ethylene/norbornene copolymers is extremely sensitive to the catalyst used[12] and there is no linear correlation between the amount of norbornene incorporated in copolymers and its thermal behavior at high incorporation. The mechanical properties otherwise are modified with the content of norbornene.[13–16] Synthesis of isotactic propylene/norbornene copolymers or ethylene/norbornene/1-hexene terpolymers synthesized by metallocen catalysts has also been published with similar tendencies regarding the lower catalytic activities and the higher T_gs of the resulting material.[17–20]

The synthesis of syndiotactic propylene copolymers with cyclic groups has been rarely published and most of these reports used norbornene as a comonomer.[11,21–24] Kaminsky et al.[11] showed that is possible to obtain these copolymers with metallocene catalysts. The novel syndiotactic copolymers displayed a broad range of T_gs depending on the amount of norbornene incorporated. However, the molecular weight of the polymers is dramatically decreased with the comonomer incorporation. Depending on the metallocene used, the catalyst activity can also decrease with the presence of the comonomer as the entrance of propylene units after the incorporation of a norbornene molecule is difficult.[11] The last issue is relevant as in general syndio-specific catalysts present lower activities and incorporations than iso-specific ones.[13] Regarding the properties of the resulting copolymers, the main focus has been the relationship between the comonomer content and the T_gs of the copolymer, without further details about other properties. Not only there is a lack of studies about copolymer properties but also about the effect of adding nanoparticles, despite the broad range of properties that can be modified by this route. The addition of nanoparticles may be beneficial in these systems as sPP has lower crystallinity and crystallization rate than iPP, thus limiting its mechanical properties and commercial impact. Therefore, the addition of nanoparticles acting as nucleating agents could improve these characteristics of sPP as reported previously for clay nanoparticles.[26]

Based on the details mentioned above, the preparation of composites of syndiotactic COCs with nanoparticles can be considered as an advantageous route in order to prepare novel polyolefins. The goal of the present manuscript is to analyze the effect of two different nanoparticles (CNT and SiO_2) on the behavior of one sPP and one syndiotactic propylene/norbornene copolymer synthesized by a metallocene catalyst.

2. Experimental Section

2.1. Polymerizations

The metallocene catalyst $Ph_2C(Cp)(9\text{-}Flu)ZrCl_2$ (Boulder Scientific) was used as received. Methylaluminoxane (MAO) (10 wt/vol% in toluene) cocatalyst (Chemtura) was used without further purification. Toluene (JB Baker) was distilled over sodium under a nitrogen atmosphere. The propene was acquired from Petroquim S.A. in a purity of 99.95% and was purified by passage through three columns containing BASF catalysts R3-11G and R3-12, and a 4 Å molecular sieve, to remove oxygen, sulfur, and traces of water, respectively. Norbornene (99% purity; Aldrich) and used as a stock-solution in toluene at a known concentration. All manipulations were performed under nitrogen in a dry box or using standard Schlenk line techniques. The copolymerizations were carried out in a 1 L double-jacketed Büchi glass reactor equipped with a mechanical stirrer and thermostatically heated. The pre-activated metallocene catalyst (activated with MAO), dissolved in a small amount of toluene, was added to the reactor at a final catalyst concentration of 6×10^{-6} mol L^{-1}. The molar ratio of MAO/metallocene ([Al]/[Zr]) was equal to 1000. When the catalytic system was added to the reactor, 2 mL of norbornene was incorporated to the reactor, with a total reaction volume of 500 mL. Polymerization was initiated via the addition of gaseous propylene into the reactor. The temperature was maintained at 30 °C. The stirring rate (1000 rpm) and propene pressure (2 bar) were kept constant for all the reactions. The polymerization was allowed to proceed for a period of half hour and was terminated using a solution of acidified methanol (10% HCl) and the copolymer precipitated with acetone. The catalytic activity was expressed as the mass of polymer (kg) produced per unit time (h) per mol of Zr and per unit pressure (kg mol^{-1} bar^{-1} h^{-1}).

2.2. Nanocomposites

For the preparation of the polymer nanocomposites, two kinds of nanoparticles were used: silica nanoparticles synthesized by sol–gel method, and multiwalled carbon nanotubes (MWCNT).

Spherical silica nanoparticles of 20 nm (S20) were synthesized by the sol–gel method using a two-stage mixed semi-batch method. In the first stage, solutions A and B were prepared. For solution A, 23 mL of ethanol and 55 mL of TEOS were mixed whereas 23.5 mL of ethanol, 54 mL of water, and 2.2 mL of ammonia were used for solution B. Solution B was then added dropwise to solution A. The resulting mixture was allowed to react for 60 min at 40 °C under a N_2 atmosphere. In the second stage, solutions A and B were again prepared and added to the reactor containing the solution and the particles prepared in the first stage. Details can be found elsewhere.[27,28] The MWCNT were kindly supplied by Bayer Material Science AG (Baytubes C150P). Based on the datasheet information provided by Bayer, they are characterized by a purity higher than 95 wt%, number of walls between 2 and 15, an outer mean diameter of 13–16 nm, an inner mean diameter of 4 nm, length between 1 and >10 μm, and a bulk density around 150 kg m^{-3}. The composites were prepared by using a Brabender plasticorder internal mixer at 190 °C and with a speed of 110 rpm during 10 min. Predetermined amounts of the nanoparticles, antioxidant, and neat polymer were mixed under nitrogen atmosphere in order to obtain composites with 4 wt% of nanofiller.

2.3. Materials Characterization

The molecular weight of the polymers was determined by gel permeation chromatograph (GPC) using a Waters Alliance model 2000 GPC. The comonomer content in the copolymers was determined by ^{13}C NMR spectroscopy in a Varian Innova 300 spectrometer operating at 75 MHz.

Before the different tests, the samples were press molded at 190 °C with 50 bar of pressure for 5 min and cooled under pressure by flushing the press with cold water.

The thermal properties were analyzed using a TA Q100 differential scanning calorimeter (DSC) connected to a cooling system and calibrated with different standards. The sample weight ranged from 5 to 7 mg. Samples were heated from −45 to 200 °C at a heating rate of 20 °C min^{-1}. For crystallinity determinations, f_c^{DSC}, a value of 159 J g^{-1} was taken as the enthalpy of fusion of 100% crystalline sPP.[29] This value is considered more reasonable than the one reported previously[27] (196.6 J g^{-1}), since it has been estimated from actual values of both the DSC enthalpy of fusion and the X-ray crystalline content.

The tensile properties were measured using an HP D500 dynamometer at a rate of 6 mm min^{-1} at 23 °C. The samples were cut with a stainless steel mold with dimensions according to type IV (ASTM D638) with 1 mm of thickness.

The flexural properties were measured using a mechanical universal testing machine INSTRON model 3369 at a cross-head speed of 0.5 mm min^{-1}, according to the ASTM D790. The samples were cut with a stainless-steel mold with dimensions 80 mm × 10 mm and a thickness of 0.2 mm. The melt viscoelastic properties of the samples were obtained in an ARES rheometer from TA Instruments using parallel plate configuration with a diameter of 25 mm, at a temperature of 190 °C. Oscillatory shear experiments in the linear regime were conducted in a frequency range from 10^{-2} to 10^2 rad s^{-1}, under nitrogen atmosphere. Samples for permeability testing were produced by melt pressing the samples at 190 °C to a thickness of approximately 0.20 mm. Circles (ca. 2 cm diameter) were cut out from the initial films to fit into the permeability cell. Details about the measurements and techniques can be found elsewhere.[31]

A Vickers indentor attached to a Leitz microhardness (MH) tester was used to perform microindentation measurements. The experiments were carried out at 25 °C, with contact load of 0.98 N and 25 s. MH values (MPa) were calculated according to the following relationship:[32,33]

$$MH = 2\sin 68(P/d^2)$$

where P (N) is the contact load and d (mm) is the diagonal length of the projected indentation area.

The dynamic mechanical thermal analysis (DMTA) was performed with a Polymer laboratories MK II dynamic mechanical analyzer working in tensile mode. The temperature dependence of the storage modulus (E'), and loss tangent ($\tan\delta$) was measured at 3 Hz over a temperature range from −140 °C to 140 °C at a heating rate of 1.5 °C min^{-1}.

3. Results

3.1. Synthesis of the Polymers

Table 1 shows the main results coming from the synthesis of sPP and its copolymer with norbornene. Relevant changes are observed in the catalytic behavior due to the presence of the cyclic comonomer. As reported previously,[11,13] the presence of norbornene decreases both the catalytic activity and the molecular weight of the polymer. The bulky characteristic of the comonomer explains the drop in the catalytic activity as the insertion of a monomer unit into a metal-tertiary carbon bond formed after norbornene insertion is sterically hindered.[11,13] A similar drop in the activity was reported using similar catalytic systems.[11] The decrease by a factor of 10 in the polymer molecular weight is due to termination transfer reactions promoted by the presence of the comonomer.[34,35] This phenomenon has been previously observed in the copolymerization of either linear or cyclic olefin

Table 1. Main results for the catalytic synthesis of the analyzed samples.

Sample	Norbornene incorporation [mol%]	Activity [kg mol^{-1} bar^{-1} h^{-1}]	$\bar{M}_w$ [kg mol^{-1}]	$\bar{M}_w/\bar{M}_n$	Tacticity [% -r-]
sPP	0	17 150	400	1.9	95.6
NsPP	1.4	3950	40	2.1	94.4

comonomers.[23,36,37] Changes in the polymer molecular weight will have consequences on the properties of the material, adding another variable in the discussion about the properties of copolymer-based materials (see below for details). The propylene/norbornene copolymer is less syndiotactic than the homopolymer likely due to the presence of the norbornene enhancing the frequency of back-skips. The latter process is one of the primary causes of stereoerrors when Cs-symmetric metallocene/MAO catalysts are used.[23]

3.2. Characterization of the Polymer Matrices

Syndiotactic polypropylene has been extensively studied in materials science because of its complex polymorphism having technological consequences such as high non-linear reversible deformation.[5] sPP displays at least four limited/ordered crystal structures or polymorphisms, depending on the crystallization conditions and the stereoregularity of the polymer.[5] The so-called Form I is the most stable crystalline structure and it is characterized by one orthorhombic unit cell with chains in the s(2/1)2 antichiral helical conformation, having either ordered or disordered structures. The meta-stable Form II has a similar structure as Form I but with an isochiral conformation, whereas Forms III and IV present chains in transplanar and ($T_6G_2T_2G_2$) conformation, respectively.

Our sPP sample displays a disordered Form I polymorph, as observed in Figure 1 where its X-ray diffraction profile is shown. The (010) reflection at $2\theta = 15.9°$ is observed whereas the (211) reflection at $2\theta = 18.8°$ is completely absent, confirming the disordered Form I structure. Polymers with larger amount of defects coming directly from the reactor, without any processing, can display the Form II as previously reported.[5,29,38,39] Regarding the copolymer, Figure 1 shows that it presents the same diffraction pattern as sPP, showing that both the presence of low amount of cyclic units and the decrease in molecular weight do not modify the crystalline structure of the polymer. Figure 2 and 3 show the first and second DSC melting scans, respectively, for sPP and NsPP that are summarized in Table 2. From these data are clear the effect of the polymer microstructure and the crystallization conditions on the overall thermal behavior. During the first melting, both samples present an endothermic process around 50 °C showing an annealing effect owing to the fact that the samples were left for several days at room temperature that is higher than the T_g of the polymers. Because of this room temperature annealing, the fraction of the sample crystallized during processing into rather small and imperfect crystallites is able to melt and recrystallize before the analysis. In such cases, two different endothermic processes are observed: one at low temperature associated

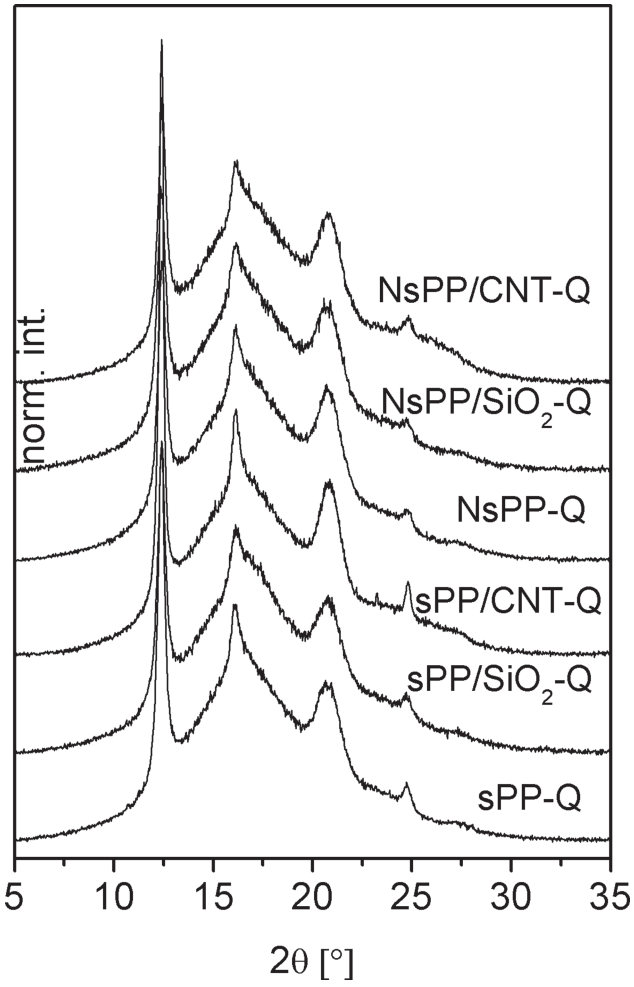

Figure 1. X-ray patterns for the different polymer matrices and composites.

with the annealing process and another one at high temperatures corresponding to the main melting process. During the second heating scan otherwise, this low temperature endothermic process formed by room temperature annealing is not observed although both samples display a main high temperature process with a double melting peak.

In order to obtain deeper information about the double melting peak, the samples were crystallized from the melt under several crystallization rates, from 1 to 40 °C min^{-1}, and the subsequent melting process, on heating at 20 °C min^{-1}, was analyzed. At low crystallization rates, stable crystals with high melting temperatures are produced whereas at high crystallization rates, only meso-stable crystal structures with lower melting temperatures are formed as polymer molecules do not have time enough to form stable crystals. Figure 4 shows some examples of the crystallization rate effect on the whole endothermic thermal behavior of the sample, whereas Figure 5 displays the changes in the melting

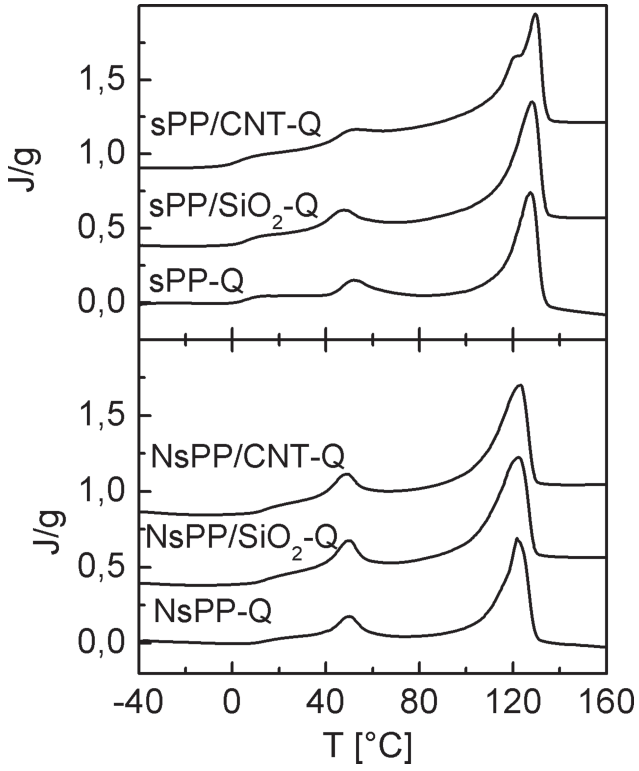

Figure 2. First heating scans for the different samples rapidly cooled from the melt. Heating rate at 20 °C min^{-1}.

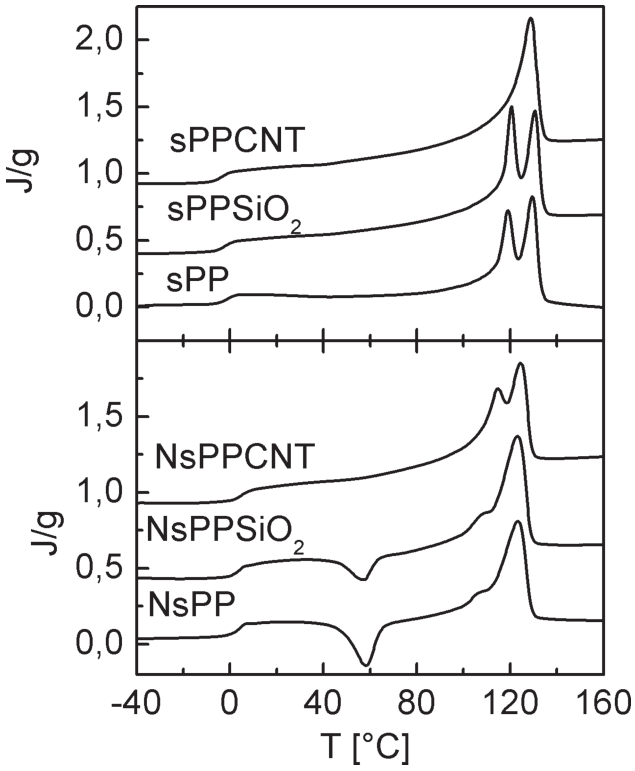

Figure 3. Second heating scans for the different samples (heating rate 20 °C min^{-1}) after non-isothermal crystallization from the melt at 20 °C min^{-1}.

temperatures for each crystallization condition. From Figure 4, it is clear that sPP crystallized at very low rate presents only one peak and that by increasing the crystallization rate two melting peaks appear. In the latter case, the low-temperature endothermic process is related with the melting of meso-stable crystals formed during the high cooling rates. Immediately after this melting process and overlapped with it, an exothermic process occurs (re-crystallization) forming more stable crystals that melt afterward, explaining the high-temperature endothermic peak. This melt/re-crystallization/re-melt (MRCRM) processes is confirmed by a non-reversible exothermic peak found in similar samples under temperature modulated DSC analysis.[38] The MRCRM process of this sample is further confirmed by observing Figure 5 where it is clearly shown that the low endothermic peak temperature changes considerably with the crystallization rate. On the contrary, the high temperature peak is almost non-sensitive to the crystallization rate, as it is formed by re-crystallization and re-melt during

Table 2. Summary of the thermal behavior of the samples and its composites with nanoparticles as measured by DSC: glass transition, T_g, melting temperature, T_m, enthalpy of melting, ΔH_m, and degree of crystallinity, f_c (for both the first melting, F1, after rapid cooling from the melt, and second melting, F2, after crystallization at 20 °C min^{-1}), and crystallization temperature, T_c.

Sample	T_g^{F1} [°C]	T_m^{F1} [°C]	ΔH_m^{F1} [J g^{-1}]	f_c^{F1}	T_c [°C]	T_g^{F2} [°C]	T_m^{F2} [°C]	ΔH_m^{F2} [J g^{-1}]	f_c^{F2}
sPP	5.5	127.5	49.3	0.31	74.5	−1.5	119.1/129.5	45.8	0.29
sPP/SiO_2	6	128.1	51.1	0.32	79.0	−2.5	120.6/130.4	44.4	0.28
sPP/CNT	3	129.5	56.9	0.36	99.5	−3.5	128.8	44.8	0.28
NsPP	13	122.8	42.3	0.27	59.0	3.5	105.5/123.2	22.3	0.14
NsPP/SiO_2	14	123.0	51.9	0.33	60.0	4	107.0/123.2	32.1	0.20
NsPP/CNT	14.5	123.2	48.5	0.31	79.0	5	114.5/124.4	41.3	0.26

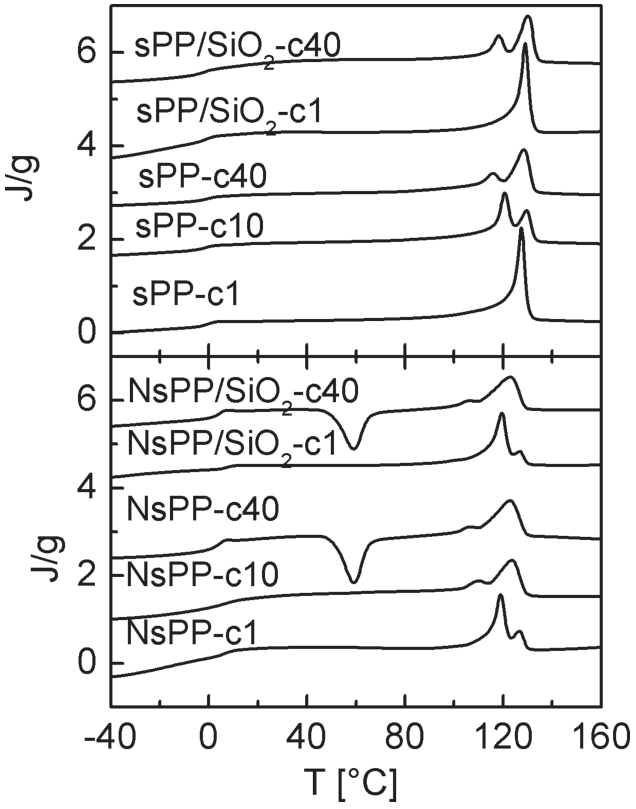

Figure 4. Representative examples of the crystallization rate effect on the subsequent heating (at 20 °C min^{-1}) of selected samples. The number after **c** indicates the cooling rate in °C min^{-1}.

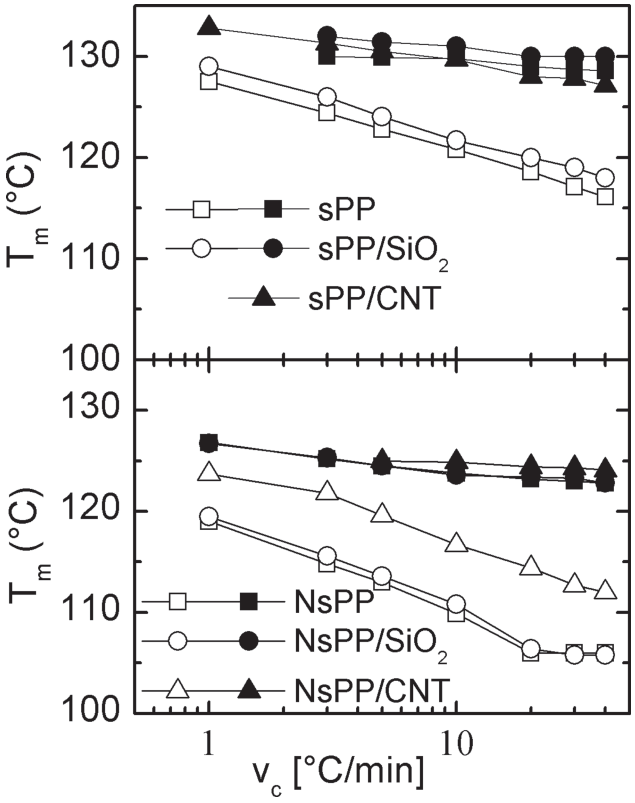

Figure 5. Effect of the crystallization rate on the melting temperature of all samples. Open symbols correspond to the temperature of the lower peak in the melt process and the full symbols, to the peak at higher temperature.

heating.[40,41] Figure 6 confirms the effect of the crystallization rate on the polymer behavior, in particular on the crystallization temperature. As above discussed, at high crystallization rates, the crystals formed are not as stable as those crystallized at lower cooling rates, explaining the inverse relationship between crystallization rate and crystallization temperature.

Regarding the copolymer, Table 2 and Figure 3 show that when the cyclic comonomer is incorporated, increasing the number of defects, the whole endothermic process is decreased and shifted to lower temperatures. These defects come from the bulky norbornenes that are excluded (at least partially) from the polymer crystals, decreasing the melting temperature of the polymer, as reported by Flory.[42] Moreover, the MRCRM process is highly changed in the copolymer due to the increased amount of defects.[5,43,44] These defects form unstable crystals that are responsible for the MRCRM process even when the sample crystallized at the lowest cooling rate (Figure 4).[34,35] The dependence between the melting temperatures and the crystallization rate is practically the same as in sPP (Figure 5). Figure 3 also shows an exothermic peak during the second heating in the copolymer associated to an irreversible cold crystallization from macromolecular segments not able to crystallize during cooling.[38] The latter is confirmed observing Figure 4 as this sample crystallized at low cooling rates does not display the exothermic process during the subsequent heating due to polymers have enough time to crystallize completely during the slow cooling. This cold crystallization is not found in iPP but it had been previously reported in sPP.[45,46] It occurs when the polymer has certain amount of defects as highly sPP do not show it whereas polymers with high defect content are amorphous. With the incorporation of defects in the polymer main chain, the crystallinity and its rate decrease, especially in polyolefins.[47,48] Therefore, when the number of defects is high enough the sample does not crystallize from the melt during cooling at usual rates, because of the short time between the melt state and the T_g. Moreover, in sPP, the cooling scan can increase the total number of activated nuclei acting as predetermined homogeneous nuclei in the subsequent heating scan, which greatly enhances the overall crystallization rate from the glassy state.[38,41] The above mentioned explains the strong cold crystallization found it in this copolymer.

Although the thermal behavior of NsPP was discussed based on the presence of norbornene, its low molecular

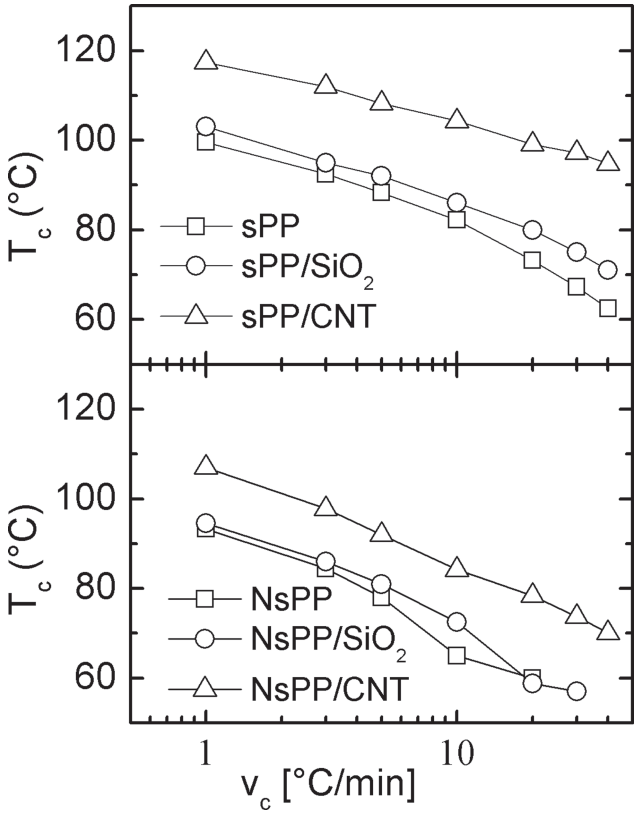

Figure 6. Effect of the cooling rate on the crystallization temperature for the different samples.

weight, as compared with sPP, could also contribute to explain the experimental findings. To better understand the real effect of the comonomer, the results from sPP and NsPP are compared with those from two syndiotactic propylene homopolymer samples reported previously by our group with similar both molecular weights ($\overline{M}_w \approx 100\,000$ and 300 000 g mol^{-1}) and syndiotacticities ($r \approx 95\%$).[38] In syndiotactic homopolymers, the decrease by a factor of three in the molecular weight did not affect the melting temperatures but increase the crystallization temperature from 68 to 80 °C as low viscosities facilitate the crystallization processes. In our case, NsPP has lower crystallization and melting temperatures than the homopolymer, despite its lower molecular weight, confirming that the thermal changes are due to the presence of comonomer and not to the difference in molecular weight. Based on this comparison, we can also conclude that the cold crystallization observed in the copolymer during the second heating (Figure 3) is also due to the presence of the comonomer as low-molecular-weight homopolymers do not present this process and it is only observed in high-molecular-weight homopolymers.[38]

Despite the low amount of comonomer incorporated into the copolymer, NsPP sample shows higher T_g than sPP, increasing from 5.5 °C to 13 °C and from −1.5 °C to 3.5 °C, for the first and second melting, respectively (see Table 2). This change is also associated with the presence of the comonomer and not with the low molecular weight of the copolymer that should decrease the glass transition as reported in similar homopolymers.[38] In the latter case, the free volume around the chain ends is enhanced in low-molecular-weight polymers explaining the decreased glass temperature. It is well known that the introduction of bulky and stiff groups into the polymer backbone inhibits the mobility of the macromolecule increasing the T_g, as the present results support. Moreover, this low amount of norbonene incorporated in NsPP is able to compensate the opposite effect of its low molecular weight.

Regarding the mechanical behavior as measured under both tensile and flexion modes, Table 3 displays the main results from these samples, with the stress–strain curves for sPP presented in Figure 7. sPP displays a thermoplastic behavior with a tensile elastic modulus of 0.4 GPa and with an elongation at break around 290%. The stress–strain behavior in the plastic zone is the typical of cold-drawing process: neck formation followed by strain hardening until the break of the sample.[29] However, with the incorporation of norbornene, the mechanical response of the sample is dramatically changed as the elongation at break decreases two orders of magnitude (Table 3). In similar homopolymer samples, when the molecular weight is decreased by a factor of 3 (from 300 kg mol^{-1}

Table 3. Main results derived from the mechanical analysis.

Sample	Stress strength [MPa]	Tensile elastic modulus [GPa]	% Elongation at break [%]	Flexion elastic modulus [GPa]	MH [MPa]
sPP	18 ± 2	0.4 ± 0.1	350 ± 50	0.5 ± 0.1	47 ± 1
sPP/SiO$_2$	28 ± 2	0.8 ± 0.1	10 ± 5	1.4 ± 0.1	52 ± 1
sPP/CNT	30 ± 2	0.8 ± 0.1	15 ± 5	1.5 ± 0.1	61 ± 1
NsPP	9 ± 1	0.5 ± 0.2	2 ± 0.5	0.7 ± 0.1	67 ± 1
NsPP/SiO$_2$	7 ± 1	0.5 ± 0.2	1.5 ± 0.5	0.6 ± 0.1	66 ± 1
NsPP/CNT	7 ± 2	0.5 ± 0.2	1.5 ± 0.5	0.7 ± 0.1	68 ± 1

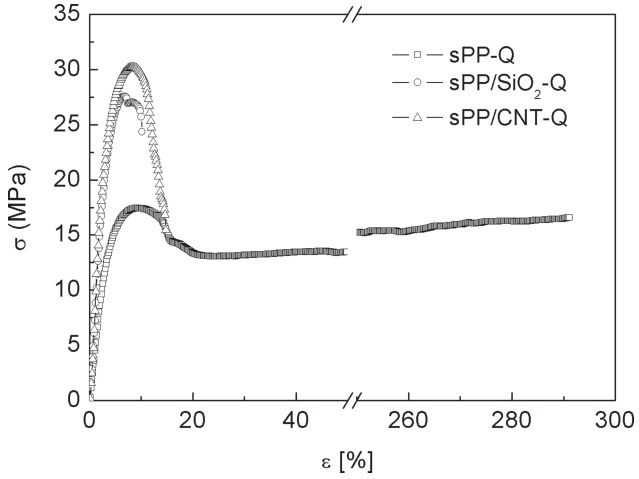

Figure 7. Stress–strain curves for sPP homopolymer and its two nanocomposites, rapidly cooled from the melt. Strain rate of 0.67 min^{-1}.

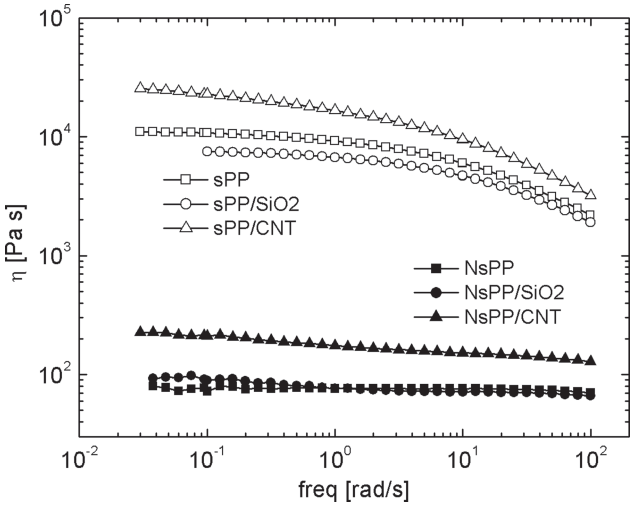

Figure 8. Dynamic viscosity of the different samples as measured under small amplitude oscillatory shear.

to 90 kg mol^{-1}), the elongation at break also decrease but only one order of magnitude: from 217% to 38%.[38] Therefore, the decrease of molecular weight (see Table 1) explains the brittle behavior of NsPP although, we can hypothesize based on the increased T_g, the presence of copolymer can further contribute. In fact, although NsPP has lower crystallinity than sPP, the presence of the bulky and stiff comonomer seems to compensate this effect in the linear zone and the elastic modulus is almost unchanged, or even slightly higher, in the copolymer, as observed in Table 3. Otherwise lower crystallinity should decrease the elastic modulus as reported in similar samples.[38] The same behavior is also obtained under flexion conditions. As the copolymer becomes brittle, it breaks before reaching the yield point and the stress strength decreases.

Microhardness is another significant mechanical property in polymers measuring the resistance of the material and involves a complex combination of properties (elastic modulus, yield strength, strain hardening, and toughness).[32,33,49,50] MH tests also provide a rapid evaluation of variation in mechanical properties affected by changes in chemical or processing conditions. In addition, MH results can be related to mechanical properties such as the elastic modulus and yield stress. The MH variation with the presence of norbornene is detailed in the last column of Table 3 confirming the trend in the elastic modulus obtained by both tensile and flexion modes.

Figure 8 shows the melt rheological behavior of the samples under small amplitude oscillatory shear conditions, in particular the dynamic viscosity. It is observed that with the incorporation of the comonomer the viscosity in the low range of frequencies decreases two orders of magnitude as compared with sPP. Moreover, the shear thinning behavior is also modified and it is shifted to larger frequencies when the comonomer is incorporated not been observed in NsPP at the range of frequencies used. The low-molecular-weight of NsPP can partially explain these results as there is a relationship between the viscosity and the molecular weight with a power of 3.4 in these systems. In this context, a decrease by a factor of 10 in the molecular weight (see Table 1) means a drop of a factor of 2500 in the viscosity at zero shear rate. The observed decrease by a factor of 100 in Figure 8 indicates that the incorporation of a bulky molecule should be further considered.

A DMTA has been carried out for sPP homopolymer. Unfortunately, the copolymer, NsPP, is very brittle and it was impossible to measure it. Figure 9 shows plots of storage and loss moduli and tanδ as a function of temperature for sPP homopolymer. Two clear relaxations are observed, ascribed to the β and γ relaxation processes. Those two relaxations are identified from the maxima in either E'' or tanδ plots, but also as two drops in the storage modulus, E': a small one at low temperature associated with the γ relaxation, and another deep fall identified with the β relaxation at higher temperatures. No evidence exists about the α relaxation at temperatures above the glass transition (β mechanism). The origin of the α relaxation is not clear, although in a previous work it was detected and associated to the crystalline phase[45]. The β relaxation is identified with the glass transition of sPP, related to generalized motions in the amorphous region, with intensity and location depending on the presence of crystalline phase. The intensity of tanδ for the present sPP sample (0.15) corresponds to a semicrystalline polymer (tanδ amorphous phase > 1.2).[45,51] The γ relaxation is

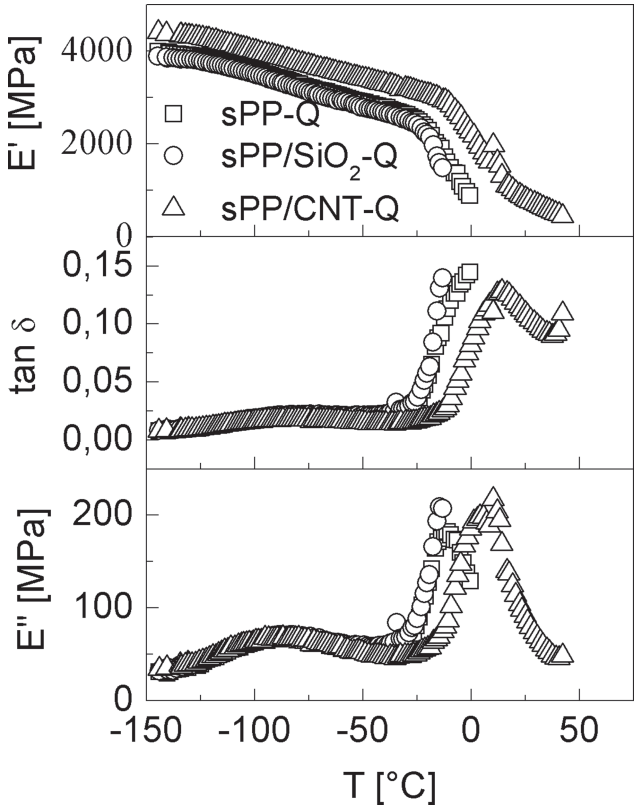

Figure 9. Dynamic mechanical thermal analyses for sPP and its nanocomposites with SiO_2 and CNT, at 3 Hz.

observed in Figure 9 at around −80 °C attributed to local motions of methyl groups directly connected to the main backbone in sPP and its copolymers.[45,51] This relaxation is quite less broad than that with similar molecular origin found in iPP.

3.3. Characterization of the Polymeric Composites

The effect of the different nanoparticles on the behavior of the syndiotactic matrices has been analyzed by the different techniques above mentioned. Thus, the X-ray diffractograms of the composites are displayed in Figure 1. Composites based on NsPP show the same behavior as those based on sPP. Similar to the pure samples, the (010) reflection at $2\theta = 15.9°$ is well observed, independently of the filler, indicating that the nanoparticles do not modify the disordered Form I structure (at least for the present concentrations). Therefore, any property change will not be related with modifications in the crystal structure of the polymers, simplifying the discussion.

Figures 2, 3, and 6 show the effect of nanoparticles on the thermal behavior of the polymer matrices as summarized in Table 2. The most noticeable effect is related to the crystallization process as nanoparticles behave as effective crystallization agents, increasing the value of T_c in more than 22 °C (with a subsequent reduction in the cold crystallization process in the second melting) as compared with the pure samples. There is also a clear effect of the kind of nanoparticle on the thermal behavior and CNT renders larger increases in T_c than SiO_2 particles (Table 2). This larger effect of CNT than SiO_2 particles is confirmed in the whole range of crystallization cooling rates as displayed in Figure 6. In the copolymer, the crystallization enhancement due to SiO_2 is practically negligible while CNT increases the value of T_c rather considerably. Moreover, no cold crystallization is observed in the second melting for the composite NsPP/CNT (Figure 3). This enhanced crystallization behavior has great consequences as these nanoparticles could solve one of the problems of sPP related with its low crystallization rate, and thus high production volumes by injection can be achieved in these composites.

Not only is the crystallization temperature modified, but also the melting behavior is, as observed in Figures 2 and 3 and summarized in Table 2. In general, nanoparticles increase the temperature of both melting peaks coming from MRCRM process, although the effect is larger in the low temperature one (Table 2). Moreover, the whole MRCRM is dramatically affected by the nanoparticles, especially for sPP matrix, and it can be reduced or even eliminated depending on the particle and the matrix. The changes observed in MRCRM confirm the results deduced from the crystallization temperatures. As above discussed, the MRCRM process is related with the presence of unstable crystals that can re-crystallize during melting. With the nanoparticles, the polymer crystals are formed easier than in the neat sample creating more stable crystals with higher melting temperatures and not able to recrystallize during heating. The relationship between the crystallization during cooling and the MRCRM is confirmed by observing that the largest changes in this process are with CNT as filler rendering the largest changes in T_c. Moreover, for sPP, the presence of CNT avoids the MRCRM process (Figure 2). The T_g otherwise is not modified by the presence of nanoparticles, as observed in Table 2, as the differences observed are in the range of the standard deviation of the measurements.

Table 3 shows the effect of nanoparticles on the mechanical behavior of the matrices. The kind of matrix is quite relevant in order to analyze the effect of the nanoparticles as concluded from this table. While sPP can increase its elastic modulus by a factor of 2 or 3, depending on the test, NsPP is not affected significantly. MH shows also the same tendency, increasing clearly in the nanocomposites based on sPP but without relevant changes in NsPP-based composites.

The strong effect of CNT nanoparticles on the mechanical tensile behavior of sPP is further confirmed in Figure 9 where the tensile dynamical mechanical thermal

analyses of these samples are shown. However, in this case, the composite sPP/SiO_2 presents the same behavior as neat sPP, whereas sPP/CNT shows significantly larger moduli in the whole range of temperatures tested. Moreover, the effect of CNT depends on the temperature. Thus, below the T_g, the composite presents an increase of around 20% as compared with pure sPP but at higher temperatures the increase is as high as 150% (close to the differences deduced from the tensile tests measured at room temperature). Interestingly, the β relaxation (glass transition) for the sPP/CNT nanocomposite is moved to a significantly higher temperature (Figure 9) although this change it is not observed by DSC (see Figure 2 and Table 2). It is important to remark that those improvements in the mechanical behavior were obtained without any kind of external agent such as a compatibilizer. Samples based on NsPP are too brittle to carry out these DMTA experiments.

Enhancements in the mechanical elastic modulus of polymer composites have been well reported previously in the case of CNT as it presents high mechanical resistance together with a high aspect ratio (≈300). For filler of low aspect ratio (≈1), such as spherical nanoparticles, no changes are expected. Therefore, the increased elastic resistance of sPP/SiO_2 composite cannot be explained by the traditional concept of load transfer from the matrix to the particle due to the non-polar characteristic of the matrix. Moreover, the nanoconfinement of the polymer matrix is not valid in our samples as the particle–particle distance is much higher than the polymer size, as shown below. In iPP composites with low concentration of SiO_2 nanoparticles, the elastic moduli are higher than those predicted by the Halpin–Tsai model as recently reported.[52,53] The entanglement of the polymer chains with the nanospheres, allowing the load transfer and increasing the stiffness of the chains surrounding the particles, was argued as the mechanism explaining this behavior.[54] This mechanism has been previously reported for single-wall nanotubes[55] and therefore can also be extended to our CNT composites, explaining also the strong stiffness improvements of this filler. The hypothesis of the entanglement of polymer chains with nanoparticles can further explain why the increase in the elastic modulus is not observed in NsPP. The size of a polymer can be estimated from the mean-square radius of gyration as:[56]

$$\langle S^2 \rangle = a \cdot M^b \; \phi = \sqrt{2 \cdot \langle S^2 \rangle}$$

where $\langle S^2 \rangle$ is the mean-square radius of gyration; M is the molecular weight of the polymer; a and b are specific constants for polypropylene, with values of 0.1296 and 1.0, respectively;[56] and φ is the diameter of the polymer. The values obtained in our samples are 22.7 and 7.2 nm for sPP and NsPP, respectively, while the diameter of the nanoparticles are 20 and 16 nm for SiO_2 and CNT. Therefore, sPP can entangle easily with the nanoparticles, whereas NsPP does not have enough size to interact with them. Changes in the crystallinity due to the presence of these particles (see Table 2) and the low stiffness of the pure matrix could further explain our tendency for sPP, as reported for polypropylene copolymers.[57] Moreover, the enhanced stiffness in sPP by the addition of nanoparticles occurs with a drastic drop in the elongation at break, as observed in Table 3 and Figure 7. Nanoparticles are able to decrease this parameter by a factor of ≈30. On the other hand, NsPP copolymer sample is already very brittle and therefore the addition of nanoparticles does not have a relevant effect on the elongation at break.

Regarding the effect of nanoparticles on the rheological behavior of the matrix in the melt state, it is concluded from Figure 8 that although there is an effect of the kind of filler, it is independent of the matrix used. In this way, SiO_2 filler does not have any relevant consequences on the dynamic viscosity in both matrices whereas CNT filler increases the viscosity at low frequencies by a factor of 2.3. In this case, the theory of the entanglement of polymer chains is still valid, although larger filler concentrations are needed to obtain a percolated system with changes in several orders of magnitude. The rheological percolation can be rationalized as arising from the comparable length of the particle–particle distances, particle size, with the polymer chains. In our case, for spherical particles, the inter-filler surface to surface distance is roughly ≈200 nm, therefore the percolation is not expected.[58] On the other hand, the high aspect ratio of CNT can explain the increase in viscosity even if the concentration is not enough for a percolation transition.[59]

Therefore, all the mechanical properties: stress–strain behavior, MH, viscoelastic measurements (DMTA and rheology) are improved by the addition of nanofiller where CNT present the largest effect.

Finally, the effect of the nanoparticles on the permeability of the samples has been studied for sPP and its composites (measurements from NsPP samples and its composites were not carried out since they are too brittle to form stable films). Figure 10 shows that at this concentration of nanoparticles there is no significant effect on the barrier properties of the specimens, despite the strong difference in the aspect ratio of the two fillers. Probably, the low amount of filler used is not enough to form a tortuosity path for oxygen molecules.[60]

4. Conclusion

A sPP and its copolymer with 1.4 mol% of norbornene (NsPP) were synthesized by a metallocenic catalyst, and

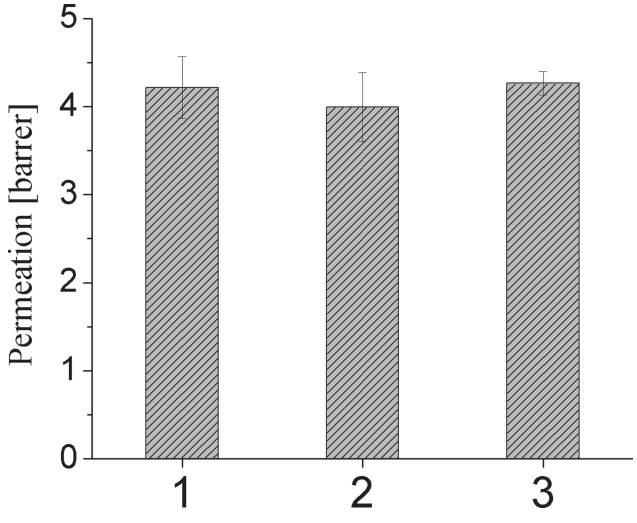

Figure 10. Permeation to oxygen of sPP sample (1) and its composites with SiO_2 (2) and CNT (3).

composites with 4 wt% of silica nanoparticles and carbon nanotubes were prepared and characterized.

Independently of the polymer structure, the pure polymers displayed the most stable sPP crystal structure of disordered Form I, and the presence of nanoparticles was not able to alter this polymorph.

Relevant effects were, however, observed in the thermal behavior, as sPP homopolymer displays an MRCRM process that is decreased, or even eliminated, by the presence of the nanoparticles. This effect is explained by the strong nucleating effect of the nanofillers, increasing the crystallization temperature and forming more stable crystals during cooling that are less affected by MRCRM process. NsPP copolymer further shows a cold crystallization on the second heating, that it is also reduced or eliminated by the presence of the nanoparticles. In general, larger changes are observed when CNT is used as a filler as compared with SiO_2 nanoparticles. This enhanced crystallization behavior has great consequences as these nanoparticles could solve one of the problems of sPP related with its low crystallization rate, and thus high production volumes by injection can be achieved in these composites.

Despite the fact that a compatibilizer was not used, a rather relevant effect of the nanoparticles is observed on the mechanical behavior of sPP, with important improvements in different mechanical parameters, depending on the filler. On the contrary, and due to the low molecular weight of NsPP, the nanoparticles do not alter significantly its mechanical behavior.

The melt rheological properties of the samples were further evaluated and a strong effect of the kind of nanoparticle was observed and CNT renders the largest increase in the dynamic viscosity of the polymer matrix.

Finally, oxygen permeation was found practically unchanged when comparing sPP and its nanocomposites. Most probably, the low amount of filler used was not enough to form a tortuosity path for oxygen molecules.

Acknowledgements: The financial support of Projects MAT2010-19883, CYTED 311RT0417 and CONICYT-CSIC 2009CL0016 is gratefully acknowledged.

Received: June 4, 2013; Revised: July 27, 2013; Published online: August 25, 2013; DOI: 10.1002/macp.201300392

Keywords: mechanical properties; nanocomposites; syndiotactic polypropylene; thermal properties

[1] P. Galli, G. Vecellio, *J. Polym. Sci.: Part A: Polym. Chem.* **2003**, *42*, 396.
[2] P. S. Chum, K. W. Swogger, *Prog. Polym. Sci.* **2008**, *33*, 797.
[3] W. Kaminsky, *Adv. Catal.* **2001**, *47*, 89.
[4] J. Huang, G. L. Rempel, *Progr. Polym. Sci.* **1995**, *20*, 459.
[5] C. D. De Rosa, F. Auriemma, *Prog. Polym. Sci.* **2006**, *31*, 145.
[6] R. C. Portnoy, J. D. Domine, in *Metallocene Based Polyolefins*, (Eds: J. Scheirs, W. Kaminsky), Wiley, New York **2000**, Ch. 22, pp. 489.
[7] G. Adriane, G. Simanke, R. S. Mauler, G. B. Galland, *J. Polym. Chem. Part A: Polym. Chem.* **2002**, *40*, 471.
[8] M. J. Yanjarappa, S. Sivaram, *Prog. Polym. Sci.* **2002**, *27*, 1347.
[9] M. D. V. Marques, D. Ramos, J. D. Rego, *Eur. Polym. J.* **2004**, *40*, 2583.
[10] W. Kaminsky, A. Laban, *Appl. Catal. A* **2001**, *222*, 47.
[11] W. Kaminsky, S. Derlin, M. Hoff, *Polymer* **2007**, *48*, 7271.
[12] J. Forsyth, J. M. Pereña, R. Benavente, E. Pérez, I. Tritto, L. Boggioni, H. H. Brintzinger, *Macromol. Chem. Phys.* **2001**, *202*, 614.
[13] T. Scrivani, R. Benavente, E. Pérez, J. M. Pereña, *Macromol. Chem. Phys.* **2001**, *202*, 2547.
[14] J. Forsyth, T. Scrivani, R. Benavente, C. Marestin, J. M. Pereña, *J. App. Polym. Sci.* **2001**, *82*, 2159.
[15] R. Benavente, T. Scrivani, M. L. Cerrada, G. Zamfirova, E. Pérez, J. M. Pereña, *J. Appl. Polym. Sci.* **2003**, *89*, 3666.
[16] N. Ekizoglou, K. Thorshaug, M. L. Cerrada, R. Benavente, E. Pérez, J. M. Pereña, *J. Appl. Polym. Sci.* **2003**, *89*, 3358.
[17] W. Kaminsky, M. Hoff, S. Derlin, *Macromol. Chem. Phys.* **2007**, *208*, 1341.
[18] L. Boggioni, A. Ravasio, A. C. Boccia, D. R. Ferro, I. Tritto, *Macromolecules* **2010**, *43*, 4543.
[19] L. Boggioni, C. Zatnpa, A. Ravasio, D. R. Ferro, I. Tritto, *Macromolecules* **2008**, *41*, 5107.
[20] L. Boggioni, I. Tritto, M. Ragazzi, P. Carbone, D. R. Ferro, *Macromol. Symp.* **2004**, *218*, 39.
[21] I. Tritto, L. Boggioni, D. R. Ferro, *Coord. Chem. Rev.* **2006**, *250*, 212.
[22] T. Hasan, T. Ikeda, T. Shiono, *Macromolecules* **2005** *38*, 1071.
[23] M. E. Vanegas, R. Quijada, G. B. Galland, *Polymer* **2010**, *51*, 4627.
[24] N. Naga, Y. Imanishi, *J. Polym. Sci.: Part A: Polym. Chem.* **2003**, *41*, 441.
[25] Z. Cai, R. Harada, Y. Nakayama, T. Shiono, *Macromolecules* **2010**, *43*, 4527.
[26] H. Palza, A. Zurita, *J. Appl. Polym. Sci.* **2012**, *124*, 2601.
[27] H. Palza, J. Vera, M. Wilhelm, P. Zapata, *Macromol. Mater. Eng.* **2011**, *296*, 744.

[28] K. Kim, H. J. Kim, *J. Sol-Gel Sci. Technol.* **2002**, *25*, 183.
[29] E. López Moya, J. M. Gómez-Elvira, R. Benavente, E. Pérez, *E-polymer* **2012**, 43.
[30] S. Hafka, K. Könnecke, *J. Macromol. Sci., Part B: Phys.* **1991**, *30*, 319.
[31] V. N. Dougnac, R. Alamillo, B. C. Peoples, R. Quijada, *Polymer* **2010**, *51*, 2918.
[32] D. Tabor, *The Hardness of Metals*, Clarendon Press, Oxford, UK **1951**.
[33] F. J. Baltá Calleja, *Adv. Polym. Sci.* **1985**, *66*, 117.
[34] R. Quijada, J. Dupont, M. S. Lacerda, M. Rosângela, B. Scipioni, G. B. Galland, *Macromol. Chem. Phys* **1995**, *196*, 3991.
[35] H. Palza, T. Velilla, R. Quijada, *Polym. Plast. Technol. Eng.* **2006**, *45*, 1233.
[36] N. Luruli, L. C. Heinz, V. Grumel, R. Brull, H. Pasch, H. G. Raubenheimer, *Polymer* **2006**, *47*, 56.
[37] V. Dougnac, R. Quijada, H. Palza, G. B. Galland, *Eur. Polym. J.* **2009**, *45*, 102.
[38] M. E. Vanegas, R. Quijada, D. Serafín, G. B. Galland, H. Palza, *J. Polym. Sci.: Part B: Polym. Phys.* **2008**, *46*, 798.
[39] C. De Rosa, F. Auriemma, E. Fanelli, G. Talarico, D. Capitani, *Macromolecules* **2003**, *36*, 1850.
[40] P. Supaphol, *J. Appl. Polym. Sci.* **2001**, *82*, 1083.
[41] P. Supaphol, J. E. Spruiell, *Polymer* **2001**, *42*, 699.
[42] P. J. Flory, *Principles of Polymer Chemistry*, Cornell University Press, New York **1953**.
[43] J. Boor, E. A. Youngman, *J. Polym. Sci., Part B: Polym. Lett.* **1965**, *3*, 577.
[44] E. A. Youngman, J. Boor, *J. Polym. Sci.: Macromol Rev.* **1967**, *2*, 33.
[45] J. Arranz-Andrés, J. Guevara, T. Velilla, R. Quijada, R. Benavente, E. Pérez, M. L. Cerrada, *Polymer* **2005**, *46*, 12287.
[46] S. Graef, U. Wahner, A. Van Reenen, R. Brull, R. Sanderson, H. Pasch, *J. Polym. Sci., Part A: Polym. Chem.* **2002**, *40*, 128.
[47] J. Rodriguez-Arnold, A. Zhang, S. Z. D. Cheng, A. J. Lovinger, E. T. Hsieh, P. Chu, T. W. Johnson, K. G. Honnell, R. G. Geerts, S. J. Palackal, G. R. Hawley, M. B. Welch, *Polymer* **1994**, *35*, 1884.
[48] R. A. Alamo, A. Ghosal, J. Chatterjee, K. L. Thompson, *Polymer* **2005**, *46*, 8774.
[49] J. M. López-Majada, H. Palza, J. L. Guevara, R. Quijada, M. C. Martínez, R. Benavente, J. M. Pereña, E. Pérez, M. L. Cerrada, *J. Polym. Sci., Part B: Polym. Phys.* **2006**, *44*, 1253.
[50] J. Arranz-Andrés, R. Benavente, B. Peña, E. Pérez, M. L. Cerrada, *J. Polym. Sci., Part B: Polym. Phys.* **2002**, *40*, 1869.
[51] J. Arranz-Andrés, R. Benavente, R. Ribeiro, E. Pérez, M. L. Cerrada, *Macromol. Chem. Phys.* **2006**, *207*, 1564.
[52] -H. Palza, R. Vergara, P. Zapata, *Compos. Sci. Technol.* **2011**, *71*, 535.
[53] J. C. Halpin, *J. Appl. Phys.* **1964**, *35*, 3133.
[54] S. S. Sternstein, A. J. Zhu, *Macromolecules* **2002**, *35*, 7262.
[55] M. Mu, K. I. Winey. *J. Phys. Chem. C* **2007**, *111*, 17923.
[56] Z. Zhou, D. Yan. *Macromol. Theory Simul.* **1997**, *6*, 597.
[57] H. Palza. *Macromol. Mater. Eng.* **2011**, *295*, 492.
[58] H. Palza, R. Vergara, P. Zapata, *Macromol. Mater. Eng.* **2010**, *295*, 899.
[59] J. Bicerano, J. F. Douglas, D. A. Brune, *Polym. Rev.* **1999**, *39*, *4*, 561.
[60] A. A. Gusev, H. R. Lusti, *Adv. Mater.* **2001**, *13*, 1641.